

Diffusion Bonding of Stainless Steel to Copper with Tin Bronze and Gold Interlayers

Jiang-tao Xiong, Qing Xie, Jing-long Li, Fu-sheng Zhang, and Wei-dong Huang

(Submitted September 13, 2010)

Vacuum diffusion bonding of stainless steel to copper was carried out at a temperature ranging from 830 to 950 °C under an axial pressure of 3 MPa for 60 min with three kinds of interlayer metals: tin-bronze (TB) foil, Au foil, and TB-Au composite interlayer. The results showed that the grain boundary wetting was formed within the steel adjacent to the interface due to the contact melting between TB and Au when TB-Au composite interlayer was used. The grain boundary wetting could occur at a relatively low temperature of 830 °C and becomes significant with the increase of temperature. The tensile strength of the joint with TB-Au was higher than that with TB or Au interlayer separately and could be 228 MPa at the joining temperature of 850 °C. Furthermore, the axial compression ratio of the specimen joined at 850 °C was approximately 1.2%. Therefore, a reliable and precise joining of stainless steel to copper could be realized by diffusion bonding with the TB-Au composite interlayer at a comparatively low temperature.

Keywords contact melting, diffusion bonding, grain boundary wetting

1. Introduction

Steel-copper alloy composite structure incorporates the advantages of excellent heat conduction and wear resistance of copper alloy and high strength of steel. Several methods such as explosive bonding (Ref 1), friction welding (Ref 2), laser welding (Ref 3), and diffusion bonding (Ref 4-6) have been proposed for joining steel to copper alloy, among which diffusion bonding is characterized as a precision joining process. However, this advantage is impaired when used for the steel-copper joining. Fe-Cu is a typical immiscible system and has limited inter-diffusivity even at elevated temperatures. Consequently, the prescribed joining temperature and pressure for steel-copper joints were about $0.9T_m$ of copper alloy and 10 MPa, respectively (Ref 4, 5), which are higher than a general case ($0.7T_m$ and 2-5 MPa). Thus, the dimensional accuracy as well as the strength of the joints is damaged due to the obvious creep deformation and grain coarsening of copper alloy. Nishi and Kikuchi (Ref 7) and Kalinin et al. (Ref 8) focused on the brazing of steel to copper alloy using gold- and copper-base filler metals, respectively, and significant deformation was avoided since pressure was absent. Nevertheless,

there was still grain coarsening of copper base metal due to the high joining temperature of 930-1010 °C. In addition, the used filler metals were specially prepared (Ref 7, 8).

Therefore, the aim of this study is to investigate the possibility of decreasing the diffusion bonding temperature and pressure by inserting the commercially available tin-bronze (TB) foil, Au foil, and TB-Au composite interlayer. The interface microstructure of the diffusion bonded pure copper and stainless steel was examined and the joint strength was evaluated by tensile test.

2. Experimental Procedure

The commercially available pure copper and austenitic stainless steel (1Cr18Ni9Ti type, 0.08 wt.%C, 18.2 wt.%Cr, 9.86 wt.%Ni, 0.68 wt.%Ti, 1.23 wt.%Mn, 0.48 wt.%Si) bars were selected as base metals in this study with the dimensions of $\varnothing 50 \text{ mm} \times 100 \text{ mm}$. The used interlayer metals were 100 μm thick TB foil (QSn6.5-0.1 type, 6-7 wt.%Sn, 0.1-0.25 wt.%P), 5 μm thick pure Au (99.99 wt.%) foil. The TB-Au composite interlayer was also used with Au foil adjacent to the steel as shown in Fig. 1.

The faying surfaces were polished using emery papers up to 1500 grit and ultrasonically cleaned in distilled water prior to bonding. Similarly, the TB foil was also roughened with a 1500 grit emery paper and ultrasonically cleaned in ethanol. The bonding experiments were performed at 830, 850, 920, and 950 °C under an axial pressure of 3 MPa for 60 min. The polished cross sections of the joints were etched by a solution of 6 g $\text{FeCl}_3 + 10 \text{ mL HCl} + 90 \text{ mL H}_2\text{O}$. The microstructure and element distributions across the joining interface were analyzed by using scanning electron microscopy (SEM) equipped with energy dispersive spectrometry (EDS). The strengths of the joints were evaluated by a tensile testing machine (INSTRON 3382) at a crosshead speed of 0.5 mm/min.

Jiang-tao Xiong and Wei-dong Huang, State Key Laboratory of Solidification Processing, School of Materials Science and Engineering, Northwestern Polytechnical University, Xi'an 710072, People's Republic of China; and Qing Xie, Jing-long Li, and Fu-sheng Zhang, Shaanxi Key Laboratory of Friction Welding Technologies, Northwestern Polytechnical University, Xi'an 710072, People's Republic of China. Contact e-mails: nancyxstar@gmail.com and xieqing@mail.nwpu.edu.cn.

3. Results and Discussion

Figure 2 shows the cross-sectional microstructure of the specimens joined with the TB-Au interlayer at 830-950 °C. It can be seen that the grain boundary wetting due to the contact melting is presented on the steel side near the joining interface and becomes more significant as the joining temperature increases. It could be deduced that the contact melting between TB and Au results in the infiltration of the liquid alloy until Au foil was entirely consumed. Since Cu and Sn in the liquid alloy can remarkably reduce the grain boundary energy of the steel (Ref 9, 10), the liquid alloy will infiltrate into the steel along the austenite grain boundaries. The zoom-in micrographs for Regions B and C in Fig. 2 are shown in Fig. 3 and 4, respectively. From the concentration profiles in Fig. 3(b), it can be deduced that the composition of the infiltrating alloy

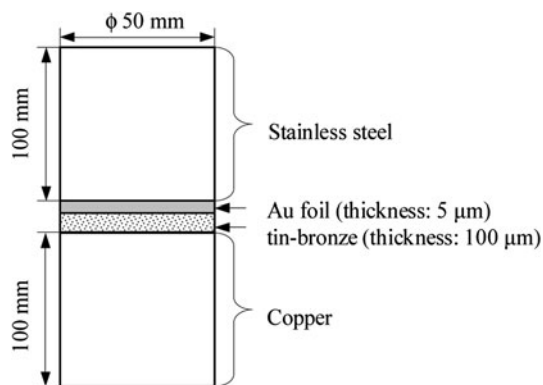


Fig. 1 Configuration of butt joint using the TB-Au composite interlayer

(Region D in Fig. 3a) is mainly Cu, Au and small amounts of Sn. The deduction was confirmed by the analysis of the composition of Points B and C (see Fig. 4) presented in Table 1. Since the main infiltrating component is Cu, the ferric chloride solution, a typical etchant for Cu alloy, was chosen. Therefore, some Cu will be removed by the etchant and then the grain boundaries are revealed, as shown in Fig. 2(c) and (d), which indicates that more liquid is infiltrated along the grain boundaries of the steel when the joining temperature increases.

Figure 5 shows the temperature dependencies of the infiltrating depths which are the average values obtained from five different positions on the steel side. The infiltrating depth increased from 2.6 to 212 μm with joining temperature increasing from 830 to 950 °C. It should be pointed out that the infiltration is discontinuous at 850 °C, and the infiltrating alloy is found inside the steel (Region A in Fig. 2b) far from the joining interface.

Figure 6(a) shows the joining interface bonded with the TB interlayer at 950 °C. The contents of Cu and Sn at Point D are 92.7 and 3.7 wt.%, respectively. According to Cu-Sn phase diagram, it can be estimated that the melting point of Point D is about 980 °C (indicated by Point 1 in Fig. 7) even without consideration of the effect of the high melting point elements (Fe, Ni, and Cr). Consequently, there is no melting occurred in the TB interlayer joint and the joining interface is straight, which is a typical morphology found in solid-state diffusion bonding.

The microstructure of the joint bonded with Au interlayer at 950 °C is shown in Fig 6(b). The lowest melting point of Cu-Au system (910° C, 20 wt.%Cu and 80 wt.%Au) is lower than the joining temperature for copper-Au-steel (950 °C). The contact melting has occurred at the interface between Au and Cu during the joining process, and thus the Au-Cu liquid alloy is in contact with the steel. The joining interface remains,

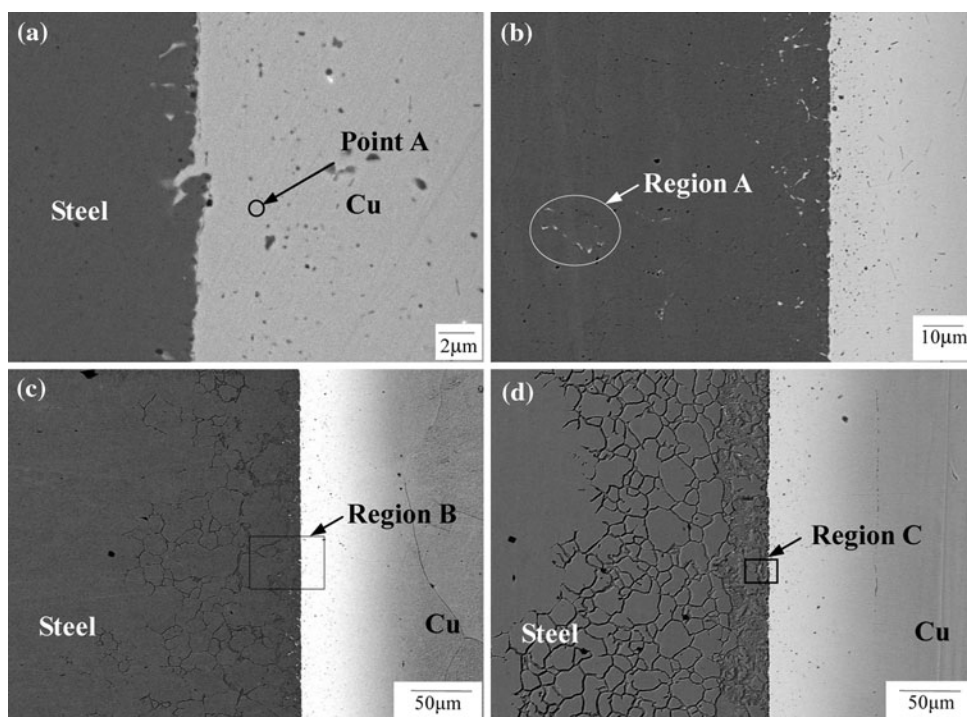


Fig. 2 SEM micrographs of the specimens joined with the TB-Au interlayer at different temperatures: (a) 830 °C, (b) 850 °C, (c) 920 °C and (d) 950 °C for 60 min

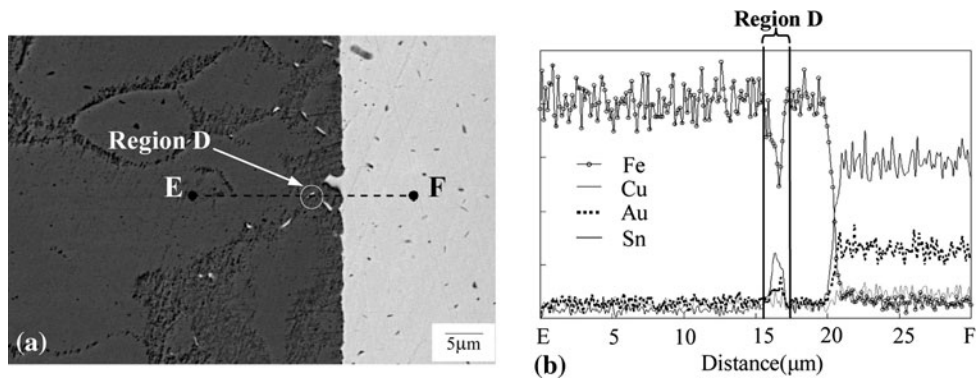


Fig. 3 EDS analysis of the joint showing (a) microstructure and (b) concentration profiles of major elements on EF line of Region B in Fig. 2(c)

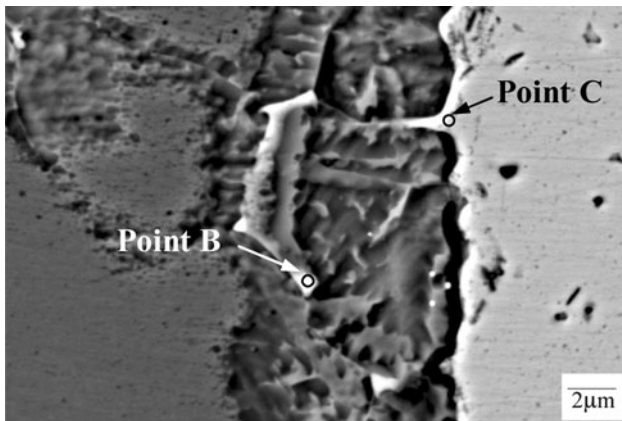


Fig. 4 SEM micrograph of Region C in Fig. 2(d)

Table 1 Chemical composition of Point A in Fig. 2(a), Points B and C in Fig. 4, and Point D in Fig. 6 (wt.%)

Point	Fe	Cr	Ni	Ti	Cu	Au	Sn	Zn
A	1.1		0.8		57.5	35.9	3.8	0.9
B	5.3	1.3	1.7	2.1	71.3	15.2	3.1	
C	13.2	3.7	2.8		60.5	16.4	3.4	
D	2.3		0.7		92.7		3.7	0.6

however, straight-like with no obvious grain boundary wetting. There may be two reasons to explain why the wetting process was hindered. First, once the liquid was formed and in contact with the steel, high melting point elements such as Fe, Ni, and Cr dissolved into the liquid alloy, which increases the melting point of the liquid over the joining temperature (950 °C) and causes the isothermal solidification of the liquid, and then the lifespan of the liquid alloy is shortened. Secondly, since the liquid alloy in the joint results from the contact melting between Au foil and copper base metal, the liquid phase is Au-rich, but too much Au will have a negative effect on the infiltrating process (Ref 7).

From comparison of Fig. 2 and 6(b), it could be found that the grain boundary wetting temperature for copper-TB-Au-steel specimen is significantly lower than that for copper-Au-steel

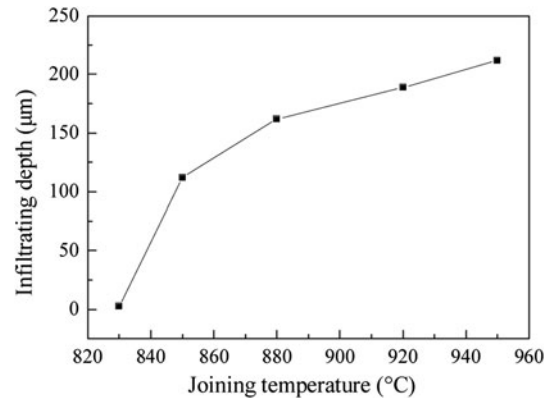


Fig. 5 Temperatures dependencies of infiltrating depths on the steel side using the TB-Au interlayer

specimen. Therefore, it can be speculated that the contact melting between TB and Au at the low temperature of 830 °C is mainly attributed to the diffusion of Sn originated from the TB into the Au foil, rather than the Au-Cu interdiffusion or the TB melting. Figure 7 shows the melting point of Cu (Au)-Sn binary system at high temperatures. It is worth noting that the melting point of Au-Sn system decreases more rapidly than Cu-Sn system with increasing Sn content. The solidus temperature for Au-Sn system with 3.8 wt.%Sn is only about 620 °C (indicated by Point 2 in Fig. 7), which can offset the negative effect of the high melting point elements such as Cu, Fe, Ni, and Cr, and results in that Point A in Fig. 2(a) (its composition is shown in Table 1) is in the liquid state during the joining process.

The tensile strengths of the specimens bonded with TB, Au, and TB-Au interlayers are shown in Fig. 8. It is indicated by the dotted line in Fig. 8 that the axial compression ratio of the joined specimen mainly depends on the joining temperature and increases from 0.6 to 4.6% with the temperature increasing from 830 to 950 °C. Since grain boundary wetting increases the bonding area, the joint with the TB-Au interlayer has the highest strength as shown in Fig. 8. If the joining temperature is low, the grain boundary wetting will be insignificant (see Fig. 2a), and if it is high, the grain coarsening will impair the strength of copper base metal. Accordingly, the specimen joined with the TB-Au interlayer at 850 °C has the maximum

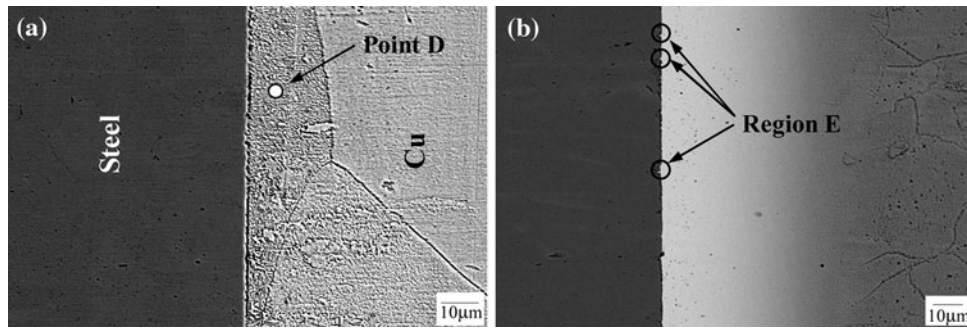


Fig. 6 SEM micrographs of the joints bonded with (a) TB and (b) Au interlayers at 950 °C for 60 min

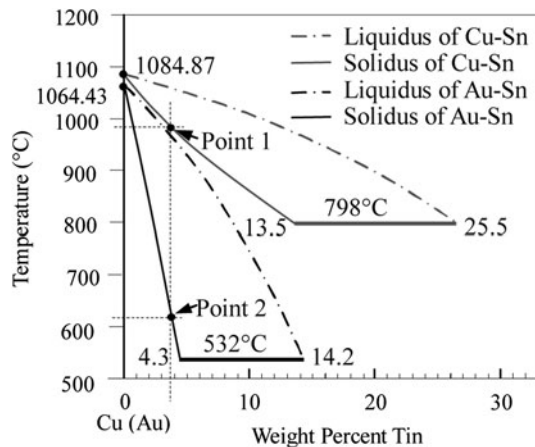


Fig. 7 Phase diagrams of Cu-Sn and Au-Sn in the Cu- and Au-rich corners at high temperatures (Ref 11, 12)

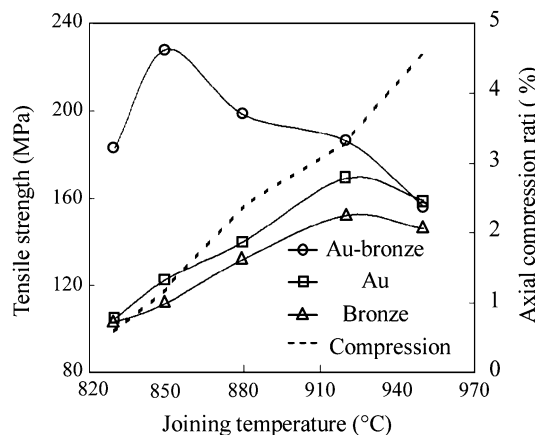


Fig. 8 Tensile strengths and axial compression ratios of the specimens joined with the different interlayers at different temperatures

tensile strength of 228 MPa and little axial compression ratio of 1.2%. The fracture of copper-TB-Au-steel specimen occurred in copper base metal, while the fracture surface of the other specimens were all located at the joining interface. The comparatively lower strengths of the joints with TB or Au interlayer indicate that the joining pressure (3 MPa) used in this experiment is insufficient for these joints, which is consistent with the report by Nishi et al. (Ref 5).

4. Conclusions

Stainless steel was diffusion bonded to copper using three kinds of interlayer metals: TB foil, Au foil, and TB-Au composite interlayer under the same parameters. The grain boundary wetting produced by the contact melting was observed in the joint with the TB-Au interlayer at above 830 °C. The infiltrating alloy along the austenite grain boundaries was produced by the contact melting between TB and Au owing to the diffusion of Sn and Cu into Au foil. Since the grain boundary wetting is beneficial to the increase of the bonding area, the strength of the joint with the TB-Au interlayer is much higher than that with other two kinds of interlayers. In addition, comparatively low pressure (3 MPa) and temperature (830-920 °C) were used in this study. The specimen with the TB-Au interlayer joined at 850 °C has the highest tensile strength of 228 MPa and little deformation (axial compression ratio of 1.2%). In particular, a new promising bonding mechanism for the steel-copper joint through grain boundary wetting within the steel base metal is discovered and could be expected to apply to the diffusion bonding of dissimilar materials.

Acknowledgment

This study was supported by the fund of the State Key Laboratory of Solidification Processing in Northwestern Polytechnical University (No. 43-QP-2009 and 31-TP-2009).

References

1. A. Durgutlu, B. Gulenc, and F. Findik, Examination of Copper/Stainless Steel Joints Formed by Explosive Welding, *Mater. Des.*, 2005, **26**, p 497-507
2. K. Tsuchiya and H. Kawamura, Mechanical Properties of Cu-Cr-Zr Alloy and SS316 Joints Fabricated by Friction Welding Method, *J. Nucl. Mater.*, 1996, **233-237**, p 913-917
3. C. Yao, B. Xu, X. Zhang, J. Huang, J. Fu, and Y. Wu, Interface Microstructure and Mechanical Properties of Laser Welding Copper-Steel Dissimilar Joint, *Opt. Laser Eng.*, 2009, **47**, p 807-814
4. H. Sabetghadam and A. Zarei Hanzaki, A. Araee, Diffusion Bonding of 410 Stainless Steel to Copper Using a Nickel Interlayer, *Mater. Character.*, 2010, **61**, p 626-634
5. H. Nishi, T. Araki, and M. Eto, Diffusion Bonding of Alumina Dispersion-Strengthened Copper to 316 Stainless Steel with Interlayer Metals, *Fusion Eng. Des.*, 1998, **39-40**, p 505-511
6. O. Yilmaz and H. Celik, Electrical and Thermal Properties of the Interface at Diffusion-Bonded and Soldered 304 Stainless Steel and Copper Bimetal, *J. Mater. Process. Technol.*, 2003, **141**, p 67-76

7. H. Nishi and K. Kikuchi, Influence of Brazing Conditions on the Strength of Brazed Joints of Alumina Dispersion-Strengthened Copper to 316 Stainless Steel, *J. Nucl. Mater.*, 1998, **258–263**, p 281–288
8. G.M. Kalinin, V.Y. Abramov, A.A. Gervash, V.B. Zolotarev, N.S. Krestnikov, I.V. Mazul, Y.S. Strebkov, and S.A. Fabritsiev, Development of Fabrication Technology and Investigation of Properties of Steel-to-bronze Joints Suggested for ITER HHF Components, *J. Nucl. Mater.*, 2009, **386–388**, p 927–930
9. T. Ishida, The Interaction of Molten Copper with Solid Iron, *J. Mater. Sci.*, 1986, **21**, p 171–1179
10. M.G. Nicholas and C.F. Old, Liquid Metal Embrittlement, *J. Mater. Sci.*, 1979, **14**, p 1–18
11. M. Li, Z. Du, C. Guo, and C. Li, Thermodynamic Optimization of the Cu-Sn and Cu-Nb-Sn Systems, *J. Alloys Compd.*, 2009, **477**, p 104–117
12. H. Okamoto, Au-Sn (Gold-Tin), *J. Phase Equilib. Diffu.*, 2007, **28(5)**, p 490